AGU100 ADVANCING EARTH AND SPACE SCIENCE

Geophysical Research Letters

RESEARCH LETTER

10.1029/2018GL079180

Special Section:
The Three Major Hurricanes of 2017: Harvey, Irma and Maria

Transient Response of the Gulf Stream to Multiple Hurricanes in 2017

Robert E. Todd[1], Taylor G. Asher[2], Joleen Heiderich[1,3], John M. Bane[2], and Richard A. Luettich[2]

[1]Woods Hole Oceanographic Institution, Woods Hole, MA, USA, [2]Department of Marine Science, University of North Carolina at Chapel Hill, Chapel Hill, NC, USA, [3]Massachusetts Institute of Technology-Woods Hole Oceanographic Institution Joint Program in Oceanography/Applied Ocean Science and Engineering, Cambridge, MA, USA

Key Points:

- A Spray glider collected multiple cross-Gulf Stream transects during the 2017 Atlantic hurricane season
- An upper ocean salinity anomaly in the Gulf Stream likely resulted from Irma-induced precipitation over Florida and the west Florida shelf
- Gulf Stream transport was reduced by as much as 40% for about 2 weeks after the passages of Hurricanes Jose and Maria

Correspondence to:
R. E. Todd,
rtodd@whoi.edu

Citation:
Todd, R. E., Asher, T. G., Heiderich, J., Bane, J. M., & Luettich, R. A. (2018). Transient response of the Gulf Stream to multiple hurricanes in 2017. *Geophysical Research Letters*, *45*, 10,509–10,519. https://doi.org/10.1029/2018GL079180

Received 13 JUN 2018
Accepted 14 SEP 2018
Accepted article online 19 SEP 2018
Published online 4 OCT 2018

Abstract Autonomous underwater glider observations collected during and after 2017 Hurricanes Irma, Jose, and Maria show two types of transient response within the Gulf Stream. First, anomalously fresh water observed near the surface and within the core of the Gulf Stream offshore of the Carolinas likely resulted from Irma's rainfall being entrained into the Loop Current-Gulf Stream system. Second, Gulf Stream volume transport was reduced by as much as 40% for about 2 weeks following Jose and Maria. The transport reduction had both barotropic and depth-dependent characteristics. Correlations between transport through the Florida Straits and reanalysis winds suggest that both local winds in the Florida Straits and winds over the Gulf Stream farther downstream may have contributed to the transport reduction. To clarify the underlying dynamics, additional analyses using numerical models that capture the Gulf Stream's transient response to multiple tropical cyclones passing nearby in a short period are needed.

Plain Language Summary In September 2017, Hurricanes Irma, Jose, and Maria impacted the Gulf Stream in rapid succession. Observations collected by an autonomous underwater glider uniquely capture the subsurface structure of the Gulf Stream during this time period, revealing two distinct transient responses of the oceanic western boundary current in the weeks following the storms. Unusually, fresh water within the Gulf Stream off the coast of the Carolinas is attributable to rain from Irma that was entrained in the Loop Current-Gulf Stream system. A reduction in Gulf Stream volume transport by as much as 40% over a period of about 2 weeks likely resulted from the hurricane-related winds over the Gulf Stream. The success of the glider mission and a submarine cable in capturing the Gulf Stream's response to passing storms highlights the need for sustained deployment of ocean observing assets to measure before, during, and after the passage of tropical systems. To clarify the underlying dynamics of the Gulf Stream's transient response to these storms, additional analyses using realistic numerical models are needed.

1. Introduction

Midlatitude western boundary currents, such as the Gulf Stream along the U.S. East Coast and the Kuroshio in the north Pacific, routinely interact with tropical cyclones. The upper ocean heat content of western boundary currents fuels tropical cyclone development (e.g., Bright et al., 2002; Galarneau et al., 2013; Nguyen & Molinari, 2012; Wu et al., 2008). Tropical cyclones also affect the western boundary currents. Upper ocean cooling in response to tropical cyclone passage has been noted near western boundary currents, but strong advection and deep thermoclines can inhibit such cooling near the axis of a western boundary current (e.g., Cornillon et al., 1987; Wright, 1969; Wu et al., 2008). Remote sensing and models have shown how near-surface oceanic flows are impacted by wind forcing (Kourafalou et al., 2016; Oey et al., 2006), while surface-to-bottom volume transport fluctuations have been measured in the Gulf Stream by a submarine cable (Ezer et al., 2017).

Storm-driven fluctuations in western boundary transport that last for days to weeks are part of the background variability upon which any longer-term trends in boundary current transport and meridional overturning (e.g., Caesar et al., 2018; Thornalley et al., 2018) are superposed. Florida Current transport reductions exceeding 40% (and three standard deviations) from the mean have been documented to persist for days to weeks after storm or frontal passage (Ezer et al., 2017; Lee & Williams, 1988; Mooers et al., 2005). Anomalous coastal sea levels associated with fluctuations in western boundary currents have been shown to drive nuisance flooding (Sweet et al., 2009) and can lead to similar or greater levels of coastal erosion than are seen

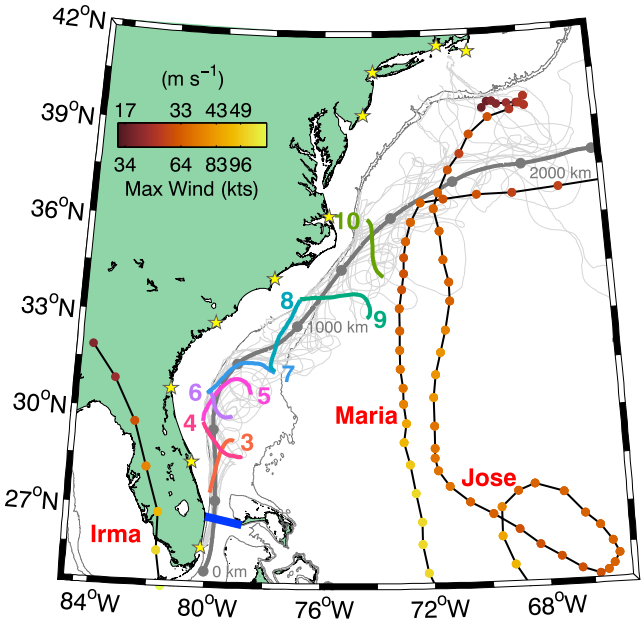

Figure 1. Locations of Gulf Stream observations and tracks of 2017 Atlantic Hurricanes Irma, Jose, and Maria. Trajectories of Spray glider surveys of the Gulf Stream from 2004 through June 2018 are shown in light gray with cross-Gulf Stream transects of interest during September and October 2017 from mission 179069 colored and numbered. The location of Western Boundary Time Series cable-based transport measurements in the Florida Straits is shown in dark blue. Best track positions of the hurricanes are shown every 6 hr with colors indicating maximum sustained wind speeds. The thick gray line is the 2004–2017 mean position of the 40-cm sea surface height contour with dots every 250 km from 25° N. Stars denote the locations of coastal tide gauge stations used here. The 200- and 1,000-m isobaths are drawn dark gray.

after a hurricane (Theuerkauf et al., 2014). The mechanisms behind these storm-driven western boundary current transport fluctuations and associated coastal sea level changes are not well understood, in part due to sparse observations within the boundary currents.

During the record-breaking 2017 Atlantic hurricane season (Balaguru et al., 2018; Rahmstorf, 2017), Hurricanes Irma, Jose, and Maria passed near the Gulf Stream in rapid succession (Figure 1). Irma made its final landfalls in the Florida Keys and near Marco Island, on the west coast of Florida, on 10 September as a Saffir-Simpson Category 4 and then 3 storm; it then decayed as it moved northward over Florida. Irma was a particularly large storm with hurricane force winds extending 130 km from the center at its final landfall. During 11–23 September, Jose completed an anticyclonic loop well east of the Bahamas, tracked northward to the east of the Gulf Stream as a Category 1 storm, and then crossed the Gulf Stream and dissipated south of New England. Maria roughly followed the northward track of Jose during 23–28 September, weakening from Category 3 to Category 1 before being swept eastward near the latitude of Cape Hatteras.

We investigate the Gulf Stream's transient response to Irma, Jose, and Maria. Section 2 describes a fortuitously timed underwater glider survey of the Gulf Stream that provides a unique view of the Gulf Stream's subsurface structure during and after passage of the storms, as well as complementary observations and reanalysis products. The observations reveal both a freshwater anomaly that is attributable to rainfall from Irma (section 3.1) and a transient reduction in volume transport (section 3.2). Section 4 summarizes the results and suggests future directions.

2. Observations and Reanalysis Data

Observations collected by a Spray autonomous underwater glider (Rudnick et al., 2016; Sherman et al., 2001) surveying across the Gulf Stream during the fall of 2017 are the focus of this analysis, and observations from 17 other Spray glider missions in the Gulf Stream that were completed between September 2004 and June 2018 and span the annual cycle (Figure 1) provide context. Spray glider number 69 was launched off Miami, Florida, for mission 179069 on 7 September 2017, 3 days before Irma made landfall in Florida and while the Miami area was under evacuation orders. Successful deployment prior to the storm was only possible

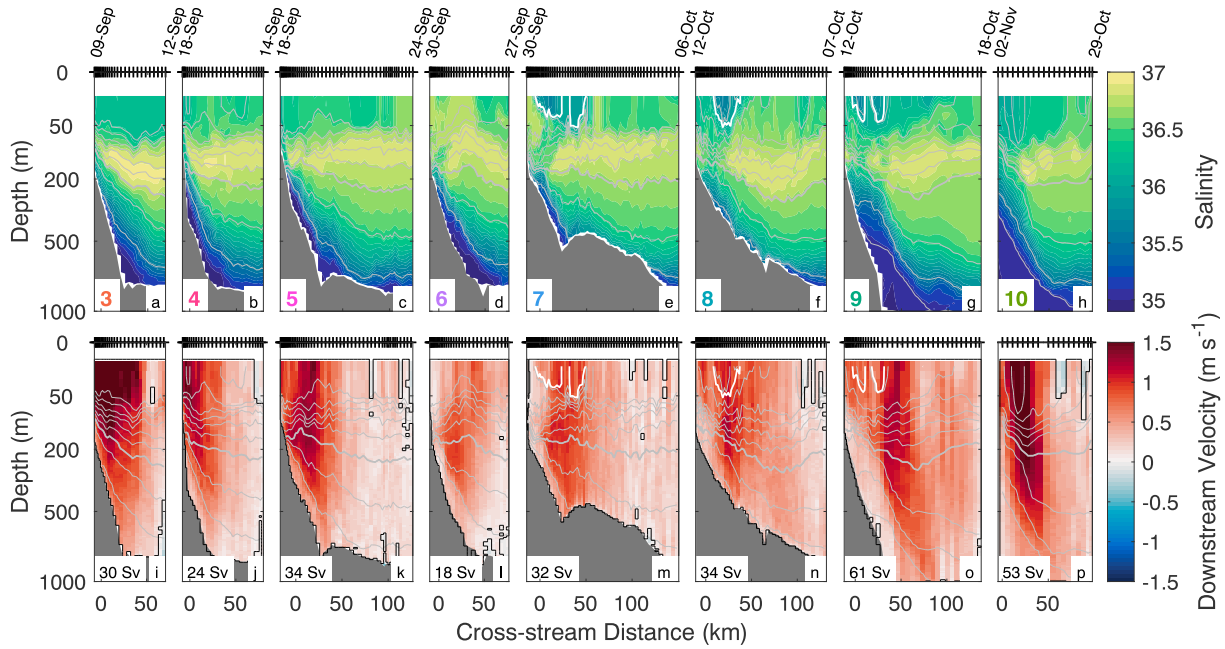

Figure 2. Cross-Gulf Stream transects of (a–h) salinity and (i–p) downstream velocity from the numbered transects in Figure 1. Gray contours are isopycnals with a contour interval of 0.5 kg/m^3 and the 26.0 kg/m^3 isopycnal bold. In (e)–(g) and (m)–(o), the 36.0 salinity contour (white) outlines the fresh anomaly. In (i)–(p), the black outline denotes the bounds of integration for estimating volume transport. Tick marks indicate the locations of individual profiles. Start and end dates of individual transects indicate the glider's direction of travel.

because the deployment-related logistics had been arranged prior to Irma threatening the region as part of an ongoing program of routine glider-based Gulf Stream surveys (Todd, 2017; Todd & Locke-Wynne, 2017). A rapid-response deployment organized once the storm was forecasted to approach the region, as our group and others have attempted in the past (e.g., Goni et al., 2017), would not have been possible.

Spray 69 crossed the Gulf Stream 10 times before being recovered offshore of North Carolina on 16 November 2017; we focus here on the last eight cross-Gulf Stream transects, numbered 3–10 (Figure 1, highlighted), which were occupied during and after Irma's passage. The glider carried a pumped Sea-Bird 41CP conductivity-temperature-depth sensor, a 1-MHz Nortek AD2CP Doppler current profiler, and a chlorophyll fluorometer. Each dive cycled from the surface to within a few meters of the seafloor or a maximum depth of 1,000 m and back to the surface; all sensors sampled on the ascending phase of each dive. Profiles of absolute horizontal velocity were estimated following Todd et al. (2017). Minor updates to the AD2CP data processing (particularly a reduction from 20 to 1 of the signal-to-noise ratio below which measurements are ignored, which reduces profile-to-profile variance) are expected to improve the root-mean-square errors in velocity profiles from the 0.24-m/s estimate for a Gulf Stream mission in Todd et al. (2017) to O(0.1) m/s, particularly near the surface where profiles are constrained to match surface velocity estimates that have accuracies of 0.05 m/s (Todd et al., 2017); profiles are constrained to match depth-average velocities that have root-mean-square errors of 0.01 m/s and negligible bias (Rudnick et al., 2018). Individual cross-Gulf Stream transects were occupied in 4–6 days (Figures 2a–2h) with a few days between successive transects as the glider maneuvered outside of the Gulf Stream. Glider observations used here are binned to a uniform vertical grid of 10-m resolution and placed in a cross-stream coordinate system (Figure 2) following Todd et al. (2016).

Other observational and reanalysis products complement the glider observations. Daily volume transport estimates from the Western Boundary Time Series (WBTS) submarine cable across the Florida Straits (Baringer & Larsen, 2001) provide high-frequency estimates of Gulf Stream transport at a fixed location. Tide gauge data from 10 stations along the U.S. East Coast between southern Florida and New England (Figure 1, stars) capture the coastal response to passing storms; the original 6-min resolution tide gauge records are low-pass filtered to remove variability at periods shorter than 1 day (e.g., tides) and then averaged hourly. Best track estimates of the eye location and maximum wind speeds for Irma, Jose, and Maria at 6-hourly intervals are obtained from NOAA's Automated Tropical Cyclone Forecast System (Sampson & Schrader, 2000). Gridded winds are

Table 1
Bulk Properties[a] of Waters Above 100 m With Salinity Less Than 36.0 for Each Cross-Gulf Stream Transect on Which Such Waters Were Encountered

Transect	Dates	Area (m^2)	Location	Salinity	Speed (m/s)
7	1–3 Oct.	1.4×10^6	31.1° N, 79.5° W	35.9	0.8
8	10–11 Oct.	9.0×10^5	32.9° N, 77.2° W	35.8	0.9
9	13–16 Oct.	7.7×10^5	33.7° N, 76.1° W	35.8	0.7
Average		1.0×10^6		35.9	0.8

[a]Properties are area-weighted averages except for dates of first and last observations.

obtained from the European Centre for Medium-Range Weather Forecasts'' ERA-Interim reanalysis product (Dee et al., 2011) at a resolution of 0.75° × 0.75°. We calculate wind stress from ERA-Interim winds following Large and Pond (1980).

3. Results and Discussion

Successive cross-Gulf Stream glider transects during September and October 2017 (Figure 2) reveal transient changes in the subsurface properties of the Gulf Stream. Since successive transects were generally farther downstream (except for transect 6, for reasons discussed below), we generally expect successive transects to have gradually reduced near-surface temperatures, increasing downstream transports (cf. Meinen & Luther, 2016; Todd et al., 2016), and weak along-stream salinity changes. Temperature (not shown) did not show any obvious deviations from these expectations (e.g., there was no marked cooling of the surface layer due to storm-induced mixing or surface heat losses) and is not discussed further, but salinity and along-stream velocity showed clear anomalies in late September and early October.

3.1. Gulf Stream Salinity Anomaly

Transects 7–9 had anomalously fresh waters in the upper 40–50 m within the core of the Gulf Stream (Figures 2e–2g). Above 100 m, salinities along transects 3–6 and 10 were always greater than 36.0 (Figures 2a–2d and 2h) while minimum salinities along transects 7–9 were near 35.6 (Figures 2e–2g); hence, we use the 36.0 isohaline shallower than 100 m to delineate the salinity anomaly (Figures 2e–2g, white contour). This salinity anomaly was first detected at the beginning of October near 31.1° N, persisted through mid-October near 33.7° N, and had largely disappeared from the glider observations by transect 10 near 35° N in early November (Table 1, Figures 2e–2h).

For transects 7–9, we calculate the cross-sectional area (i.e., normal to the vertically averaged flow) of the salinity anomaly and construct area-weighted averages of location, salinity, and downstream speed (Table 1). Averaged across transects 7–9, the salinity anomaly had a cross-sectional area of 1.0×10^6 m^2 or 1 km^2, salinity of 35.9, and speed of 0.8 m/s (Table 1). The anomaly reached transect 7 by 1 October and was still detectable at transect 9 on 16 October; subtracting 6 days for water to be advected the 425 km between transects at 0.8 m/s (Table 1) suggests that the salinity anomaly lasted at least 9 days at a given location. An equivalent along-stream length of 625 km based on the duration and speed gives an overall volume of anomalously fresh water of 6×10^{11} m^3. A simple estimate of the volume of fresh water (V_f) required to produce the observed salinity anomaly is

$$V_f = V\left(\frac{S_1}{S_2} - 1\right), \tag{1}$$

where V is the total volume of anomalous waters, S_1 is the salinity before addition of fresh water, and S_2 is the salinity of the anomalous waters after addition of fresh water and results from equating the initial mass of salt ($S_1 V$) with the final mass of salt ($S_2(V + V_f)$). Taking $S_1 = 36.4$ as the background salinity in the upper 50 m of the Gulf Stream prior to the observed salinity anomaly (e.g., Figures 2a–2d), $V = 6 \times 10^{11}$ m^3, and $S_2 = 35.9$ (Table 1), we estimate that 1×10^{10} m^3 of fresh water was required to produce the Gulf Stream salinity anomaly observed by the glider in October 2017.

The glider first detected the salinity anomaly approximately 20 days after Irma impacted the Florida peninsula. The timing of the salinity anomaly is consistent with fresh water having been advected by the O(1)-m/s flow in the core of the Loop Current (Todd et al., 2016) and Gulf Stream (Figures 2i–2p) over the O(1500) km between the west Florida shelf and coast where Irma's impacts were greatest and the location at which the

glider sampled the fresh anomaly. Thus, we posit that the observed fresh anomaly in the Gulf Stream was the result of precipitation from Irma being entrained in the Loop Current-Gulf Stream system. Atkinson and Wallace (1975) and Ortner et al. (1995) previously noted fresh anomalies in the Gulf Stream, which were produced by flood waters from the Mississippi River being entrained into the Loop Current. The quantity of fresh water required to produce the observed salinity anomaly is equivalent to 0.25 m of rain distributed uniformly over an area of 40,000 km^2, about one quarter of the state of Florida or 3 times the surface area of the observed salinity anomaly in the Gulf Stream. Irma produced in excess of 0.25 m of rain over much of the Florida peninsula (Cangialosi et al., 2018), which, when combined with rainfall over the ocean, easily accounts for the needed fresh water. Jose and Maria may have produced oceanic salinity anomalies in the Gulf Stream as well, but the glider sampling was located upstream of the tracks of Jose and Maria (Figure 1) and cannot confirm such anomalies, which would have been advected downstream.

3.2. Gulf Stream Transport Reduction

3.2.1. In Situ Observations

The Gulf Stream temporarily weakened in late September and early October of 2017. Horizontal currents measured during transects 6–9 (Figures 2l–2o) were notably weaker than preceding and following transects (Figures 2i–2k and 2p). Maximum downstream velocities (i.e., parallel to the measured depth-average velocity) for transects 6–9 were 0.9–1.3 m/s while maximum downstream velocities for transects 3–5 and 10 were 1.4–1.9 m/s. Currents were sufficiently weak in late September that transect 6 had approximately half the along-stream extent of and was located upstream from the preceding transect because the glider was not being advected downstream as quickly (Figure 1).

Gulf Stream volume transport showed a transient reduction commensurate with the observed weakening of horizontal currents. For each glider transect, we estimate the downstream volume transport T as

$$T = \int_R v \, dA, \tag{2}$$

the area integral of downstream velocity v within the cross-stream region R that bounds the Gulf Stream. The inshore and offshore ends of individual transects are chosen to be either shallower than 100 m or where gliders could navigate against the prevailing Gulf Stream direction. Within each transect, the region R is identified as a connected region of positive downstream flow (e.g., Figures 2i–2p). Our choice of bounding region therefore captures essentially all of the Gulf Stream above 1,000 m in addition to some adjacent eddy flow. While a forthcoming manuscript will address the absolute accuracy of our Gulf Stream transport estimates and time-mean along-stream trends in transport, our focus here is on the relative changes in transport between successive transects. When propagated through the transport estimate (equation (2)), random errors in glider-based velocity estimates (section 2) contribute to root-mean-square errors in transports of about 0.25 Sv for a nominal transect of 100-km extent with 20 profiles and 1,000-m vertical extent; the unlikely case of the full 0.01-m/s error in depth-average velocities being an along-stream bias would result in a transport bias of 1 Sv for the same nominal transect (Rudnick et al., 2018).

For all glider surveys across the Gulf Stream to date, the trend is for increased volume transport downstream (Figure 3a) as expected (e.g., Meinen & Luther, 2016). However, mission 179069 exhibits a minimum in transport of 18 Sv through transect 6 at the end of September; this was the lowest volume transport among 101 cross-Gulf Stream glider transects to date (Figure 3a). Compared to preceding transects from the same glider mission (e.g., 34 Sv for transect 5), volume transport during transect 6 was reduced by more than 40%. Within 2 weeks, volume transports measured by the glider recovered as current speeds increased (Figures 2m–2n), falling in the range of transports from other glider missions (Figure 3a).

Volume transport through the Florida Straits (Figure 3c) also shows reductions following storms. Ezer et al. (2017) previously noted the transport reduction following Matthew in October 2016, during which daily transport estimates remained more than one standard deviation below the long-term (2000–2017) mean (Figure 3c, shading) for 16 consecutive days with a minimum transport of 21 Sv (35% or three standard deviations below the mean). The reduction in Florida Straits transport following the 2017 hurricanes was somewhat smaller in magnitude (minimum of 24 Sv, 23% or two standard deviations below the mean) with a similar duration of 17 consecutive days with transport more than one standard deviation less than the long-term mean (Figure 3c).

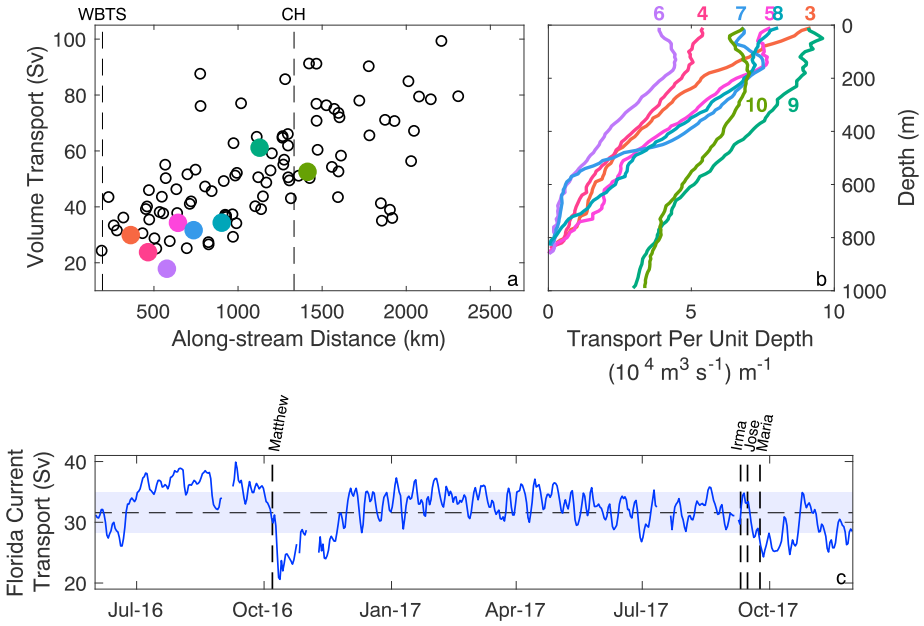

Figure 3. (a) Volume transport versus along-stream distance for all Spray glider transects that fully crossed the Gulf Stream (open circles) with transports from transects occupied during mission 179069 colored. (b) Vertical structure of volume transports from mission 179069. (c) Time series of volume transport measured by the Western Boundary Time Series submarine cable in the Florida Straits during the 2016 and 2017 Atlantic hurricane seasons with the times of closest approach of Matthew, Irma, Jose, and Maria indicated by vertical lines and the mean (31.5 Sv) and standard deviation (3.4 Sv) since 2000 indicated by the horizontal line and shading.

The glider observations uniquely capture the vertical structure of the transient reduction in Gulf Stream transport during the 2017 hurricane season. Cross-stream integration of downstream velocity from each transect gives the volume transport per unit depth (Figure 3b) with random errors from velocity profiles contributing to errors of about 2.5×10^3 (m^3/s) m^{-1} for a nominal transect with 20 profiles distributed over 100 km. The transport reduction has both barotropic (full-water column) and vertically sheared components. Transect 6, with the weakest overall transport, had reduced transport at all depths relative to all other transects, except for below 500 m on transect 7 where topography of the Charleston Bump affects Gulf Stream flow (e.g., Brooks & Bane, 1978; Gula et al., 2015; Todd, 2017). This full-depth transport reduction suggests a barotropic process influencing Gulf Stream transport. For transects 5, 6, 7, and 10, maximum transport per unit depth occurs at depths of 130–180 m rather than at or near the surface as expected for the typically sheared flow of the Gulf Stream. For transect 10, near-surface counterflow on the seaward side of the Gulf Stream results in the subsurface transport maximum (Figure 2p). For transects 5–7, however, the subsurface transport maximum results from reduced near-surface flow in the core of the Gulf Stream (Figures 2k–2m), suggesting a depth-dependent process contributing to the transient Gulf Stream slow down.

3.2.2. Potential Mechanisms

We now explore possible mechanisms behind the transient reduction in Gulf Stream transport during September and October 2017. That the transport anomaly immediately followed the passages of Jose and Maria strongly implicates the anomalous forcing associated with the storms, so we focus on the potential role of storm-related wind forcing in driving fluctuations in Gulf Stream transport.

Winds that blow downstream (upstream) relative to the Gulf Stream drive Ekman transport away from (toward) the coast as the Gulf Stream follows the continental slope south of Cape Hatteras, resulting in a cross-stream pressure gradient that reinforces (retards) the Gulf Stream. When a hurricane is situated to the east of the Gulf Stream, its cyclonic winds generally blow upstream, so we may expect storms tracking east of the Gulf Stream to slow the Gulf Stream and storms tracking west of the Gulf Stream to accelerate it. This potential method could only apply where the Gulf Stream follows the continental margin so that the continental slope and coast provide no-flow boundary conditions to support a pressure gradient (see Gill, 1982, section 10.9). To investigate this mechanism, we low-pass filter ERA-Interim-derived wind stress with a 72-hr cutoff to match the time scale inherent to the Florida Current transport time series (Meinen et al., 2010),

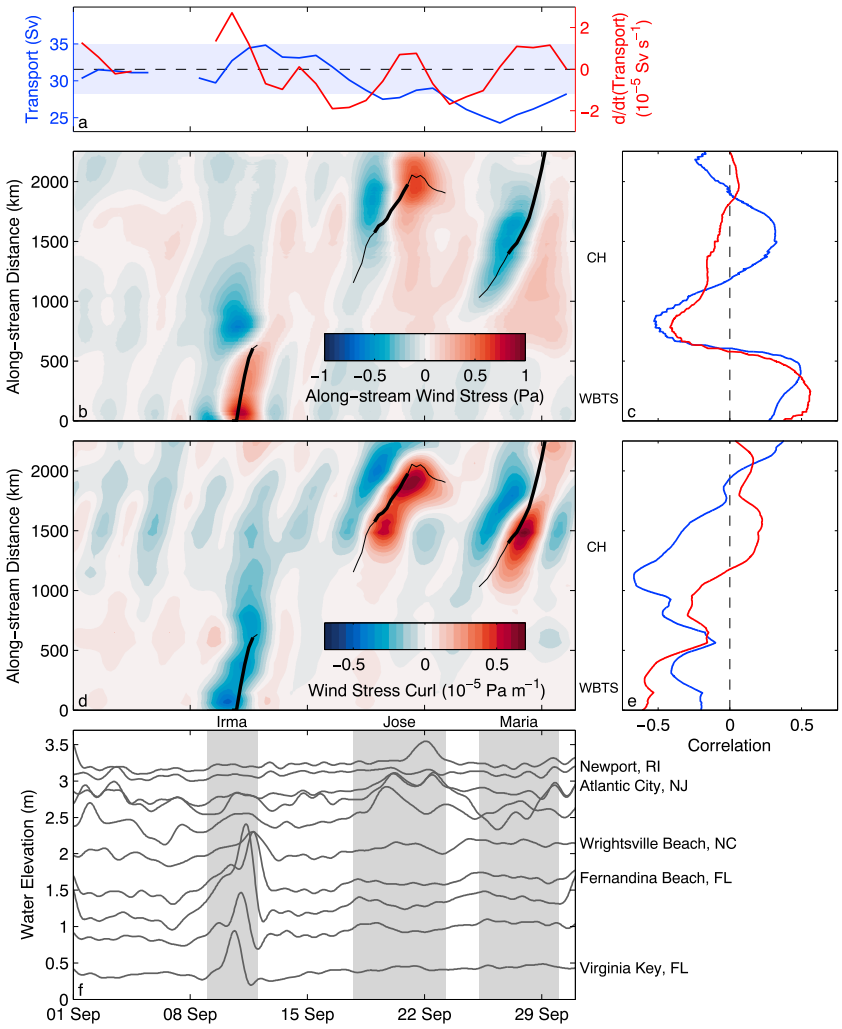

Figure 4. (a) Florida Current volume transport (blue) and its rate of change (red) during September 2017 with long-term mean and standard deviation of transport as in Figure 3c. (b) Hovmöller diagram of along-stream wind stress over the mean Gulf Stream path (Figure 1). (c) Correlations between along-stream wind stress and volume transport in the Florida Straits (blue) or its rate of change (red) at zero lag. (d) Hovmöller diagram of wind stress curl over the mean Gulf Stream path. (e) Correlations between wind stress curl and volume transport in the Florida Straits (blue) and its rate of change (red) at zero lag. In (b, d), the centers of Irma, Jose, and Maria are drawn black when within 500 km of the mean Gulf Stream path and bold when tropical storm force winds (>17.5 m/s) overlapped the Gulf Stream mean path. "WBTS" and "CH" denote the along-stream positions of the WBTS cable and Cape Hatteras, respectively. (f) Coastal water levels at selected tide gauges along the U.S. East Coast (Figure 1, stars), low-pass filtered to remove tidal signals and offset vertically proportional to the along-stream position of each gauge relative to the Gulf Stream. Shaded bands indicate the time periods during which Irma, Jose, and Maria were active in the area. WBTS = Western Boundary Time Series.

interpolate low-passed wind stress estimates onto the mean Gulf Stream path (Figure 1), and consider the stress along the local mean Gulf Stream path (Figure 4b).

The center of Irma tracked along the west coast of Florida, so its winds generally blew downstream relative to the Gulf Stream along the Florida Coast; a concurrent cold front off the Carolinas produced winds against the Gulf Stream farther downstream (Figure 4b). Jose's strongest impacts on the Gulf Stream were limited to the region downstream of Cape Hatteras (along-stream distances of 1,600–2,200 km, Figure 4b) where winds initially opposed the Gulf Stream and then blew downstream after the storm crossed the Gulf Stream around 20 September (Figure 1); Jose had a similar but weaker impact just upstream and downstream of Cape Hatteras (1,250–1,600 km). Maria's winds consistently blew upstream in the vicinity of Cape Hatteras (Figure 4b). Thus, we expect that Ekman transport away from the coast during Irma produced a pressure gradient reinforcing Gulf Stream flow while Ekman transport toward the coast during Maria produced an adverse pressure

gradient. Around Cape Hatteras (1,250–1,600 km), where the Gulf Stream is not yet far from the continental slope, Ekman transport due to Jose's winds could be expected to have driven an initially adverse pressure gradient, followed by a pressure gradient that was favorable to Gulf Stream flow.

To assess the impact of along-stream winds on Gulf Stream transport, we consider correlations between along-stream wind stress (Figure 4b) and volume transport and its rate of change through the Florida Straits (Figure 4a, blue and red, respectively) during September 2017. Correlations are calculated at zero lag at each along-stream position (Figure 4c). The short duration of the time series used here, which focus on a series of closely spaced and interrelated events, results in correlations with few degrees of freedom and consequently low statistical significance; nevertheless, the correlations are useful for identifying along-stream locations at which forcing anomalies are temporally aligned with transport anomalies measured in the Florida Straits. Positive correlations are consistent with the along-stream winds driving Gulf Stream transport variability.

Along-stream winds over the Gulf Stream along the Florida coast (along-stream distances of 0–500 km) were positively correlated with volume transport and its rate of change (Figure 4c), suggesting that winds from Irma drove an acceleration of the Gulf Stream in the Florida Straits. Such a response to local winds is in line with the simulations of winter storms by Lee and Williams (1988). Off the Carolinas (700–1,000 km), along-stream winds were negatively correlated with both transport in the Florida Straits and the rate of change of transport; these correlations are readily explained by the concurrent presence of the cold front off the Carolinas when Irma was impacting the Florida Straits. Farther downstream (1,300–1,750 km), the correlation between along-stream wind stress and Florida Straits transport has a somewhat weaker positive peak, hinting at a relationship between Jose and Maria's winds over the Gulf Stream and transport measured farther upstream; a causative relationship would require a process, such as a coastal trapped wave, to propagate the anomalous signal southward against the Gulf Stream.

Hurricanes also generate wind stress curl anomalies that can drive oceanic flows. Wind stress curl is positive (cyclonic) in the core of a hurricane, but often becomes negative (anticyclonic) around the margins of the storm (e.g., Geisler, 1970; Price, 1983). Positive wind stress curl drives Ekman divergence, upward velocity at the base of the Ekman layer, and lowering of the sea surface, producing a negative pressure anomaly throughout the water column. Geisler (1970) describes how a moving storm leaves a baroclinic ridge and barotropic trough along the storm track with flow undergoing geostrophic adjustment on the time scale of storm passage. The basic state of the Gulf Stream includes a shoreward pressure gradient force due to sea level increasing offshore, so a barotropic trough along the track of a hurricane centered over or seaward of the Gulf Stream would produce an anomalous barotropic pressure gradient in opposition to the Gulf Stream's geostrophically balanced flow. Since the Gulf Stream follows the continental margin upstream of Cape Hatteras, wind stress curl on the shoreward side of the Gulf Stream (i.e., over the shelf) is not expected to have a significant barotropic effect in deep water.

Wind stress curl along the mean Gulf Stream path shows anomalies associated with Irma, Jose, and Maria, as well as the cold front (Figure 4d), and we consider correlations between this wind stress curl and the volume transport and its rate of change through the Florida Straits (Figure 4e) as with along-stream wind stress above; negative correlations are consistent with positive wind stress curl anomalies driving reduced transport. Irma produced negative wind stress curl anomalies over the Gulf Stream along the Florida coast (0–500 km), consistent with only the outer edge of the storm impacting the Gulf Stream. Both Jose and Maria produced negative wind stress curl anomalies followed by stronger positive curl anomalies as they moved closer to the Gulf Stream. The cold front off the Carolinas around 11 September produced a negative wind stress curl anomaly that overlapped in along-stream position (near 1,100 km) with Maria-associated anomalies later in the month. Correlations between wind stress curl and both transport in the Florida Straits and its rate of change were negative from Florida to approximately Cape Hatteras (Figure 4e). The most negative correlations occurred off the Carolinas, upstream (southwest) of Cape Hatteras (1,000–1,250 km; Figure 4e, blue), suggesting that wind stress curl from Maria and/or the cold front could have contributed to the Gulf Stream transport reduction measured in the Florida Straits. However, a mechanism for propagating the anomalous transport signal upstream is necessary (e.g., a coastal trapped wave). Negative correlations in the Florida Straits (Figure 4e, red) likely result from wind stress curl being correlated with along-stream wind stress during Irma.

The preceding examination of the relationships between wind forcing along the Gulf Stream and transport measured in the Florida Straits is limited by the short time series and sparse oceanic data; hence, the analysis is suggestive of potential forcing mechanisms rather than conclusive. There are some mismatches in the

timing of forcing events and transport variability that do not fit the proposed mechanisms. For instance, the strongest upstream wind stress and most positive curl from Maria around 27–28 September (Figures 4b and 4d) coincide with transport that, while abnormally low, is increasing rather than decreasing (Figure 4a).

For either along-stream wind stress or wind stress curl off the Carolinas to cause transport fluctuations in the Florida Straits, the signal of anomalous wind forcing must propagate upstream relative to the Gulf Stream. The coastal waveguide provides a potential means of propagating a signal toward the southwest. Interestingly, transect 6 exhibits uplifted isopycnals within the core of the Gulf Stream (Figures 2d and 2l) around 27–29 September, 2–4 days after Maria's cyclonic wind stress curl began impacting the Hatteras region (Figure 4) more than 400 km farther downstream. If this isopycnal uplift resulted from wind stress curl beneath Maria (e.g., Geisler, 1970), then that signal would have needed to propagate upstream to where the glider observed it. A propagation speed of O(2) m/s as due to baroclinic coastal trapped waves (Bane, 1980; Gill, 1982) is consistent with the timing of the observed isopycnal uplift, but a single observation of uplifted isopycnals makes definitive identification of a traveling signal in the glider observations impossible.

Tide gauge measurements (Figure 4f) have been used to detect coastal trapped waves by searching for lagged correlations between stations distributed along a coast (e.g., Chelton & Davis, 1982; Enfield & Allen, 1980). We computed windowed, lagged correlations between pairs of tide gauges along the U.S. East Coast using various lags and window sizes (not shown). During September 2017, the only propagating signal detectable from those tide gauge measurements was Irma's coastal surge, which propagated poleward at about 9 m/s, roughly the speed of the storm. If baroclinic coastal trapped waves were present and had a coastal sea level signature, then their O(2)-m/s propagation speeds should be detectable along the U.S. East Coast, where propagation from Cape Hatteras to the WBTS location should take 5–7 days. The tide gauge measurements provide no clear evidence for baroclinic waves; if baroclinic waves played a role in propagating signals, such as the isopycnal uplift in transect 6 (Figures 2d and 2l), they did not have a coastal sea level signature. Barotropic waves, with phase speeds of tens of meters per second (e.g., Bane, 1980), would be undetectable since the tide gauge data were filtered to remove the (propagating) tidal signal; we cannot conclude whether barotropic waves played a role in reducing transport in the Florida Straits.

4. Summary

Observations collected during the 2017 Atlantic hurricane season show the Gulf Stream's transient response to Hurricanes Irma, Jose, and Maria. A freshwater anomaly within the Gulf Stream off the Carolinas (Figures 2e–2g; Table 1) is attributable to rain from Irma being entrained into the Loop Current-Gulf Stream system. Gulf Stream volume transport was reduced by as much as 40% for a period of about 2 weeks following the storms (Figure 3). This transport reduction, which had both barotropic and depth-dependent characteristics, may have resulted from the combination of strong winds blowing against the Gulf Stream and the positive wind stress curl produced by the series of storms passing near the Gulf Stream in rapid succession (Figures 4a–4e). Correlations between transport through the Florida Straits and winds over the Gulf Stream off the Carolinas suggest that coastal trapped waves may have propagated anomalous signals upstream relative to the Gulf Stream, but coastal tide gauge measurements show no clear evidence of such waves (Figure 4f). With multiple storms affecting the Gulf Stream during September 2017, the impacts of the individual storms were likely superposed upon each other (Price, 1983). Further investigation is necessary, likely using numerical models, to determine the specific mechanisms by which local and remote winds may have produced the observed barotropic and depth-dependent transport anomalies, as well as to examine connections between such Gulf Stream transport fluctuations, coastal sea level anomalies, and nuisance flooding. The success of both the preplanned glider mission and the WBTS cable in capturing the Gulf Stream's response to passing storms highlights the need for sustained deployment of observing assets to measure before, during, and after the passage of tropical systems.

Acknowledgments
Patrick Deane, Larry George, Raymond Graham, and Ben Hodges at WHOI and the Instrument Development Group at the Scripps Institution of Oceanography were key to the success of the Spray glider operations. The Physical Oceanography Division at NOAA's Atlantic Oceanographic and Meteorological Laboratory (AOML), North Carolina State University's Center for Marine Sciences and Technology (CMAST), and the University of North Carolina's Coastal Studies Institute (CSI) provided support for glider deployments and recoveries. Spray glider observations in the Gulf Stream are available from http://spraydata.ucsd.edu and should be cited using the following https://doi.org/10.21238/S8SPRAY2675 (Todd & Owens, 2016). Spray glider operations were funded by the National Science Foundation (OCE-0220769, OCE-1633911), the Office of Naval Research (N000141713040), NOAA's Climate Observation Division (NA14OAR4320158), Eastman Chemical Company, WHOI's Oceans and Climate Change Institute, and the W. Van Alan Clark, Jr. Chair for Excellence in Oceanography at WHOI (awarded to Breck Owens). The Florida Current cable data are made freely available on the Atlantic Oceanographic and Meteorological Laboratory web page (https://www.aoml.noaa.gov/phod/floridacurrent/) and are funded by the DOC-NOAA Climate Program Office-Ocean Observing and Monitoring Division. Tide gauge data were obtained from the NOAA National Ocean Service's Center for Operational Oceanographic Products and Services (http://tidesandcurrents.noaa.gov). Greg Seroka (NOAA) directed us to the Automated Tropical Cyclone Forecast System data (https://ftp.nhc.noaa.gov/atcf/btk). Colormaps are from Thyng et al. (2016).

References

Atkinson, L. P., & Wallace, D. (1975). The source of unusually low surface salinities in the Gulf Stream off Georgia. *Deep Sea Research and Oceanographic Abstracts*, *23*, 913–916. https://doi.org/10.1016/0011-7471(75)90093-5

Balaguru, K., Foltz, G. R., & Leung, L. R. (2018). Increasing magnitude of hurricane rapid intensification in the central and eastern tropical Atlantic. *Geophysical Research Letters*, *45*, 4238–4247. https://doi.org/10.1029/2018GL077597

Bane, J. M. Jr. (1980). Coastal-trapped and frontal-trapped waves in a baroclinic western boundary current. *Journal of Physical Oceanography*, *10*(10), 1652–1668. https://doi.org/10.1175/1520-0485(1980)010<1652:CTAFTW>2.0.CO;2

Baringer, M. O., & Larsen, J. C. (2001). Sixteen years of Florida Current transport at 27° N. *Geophysical Research Letters*, *28*(16), 3179–3182. https://doi.org/10.1029/2001GL013246

Bright, R. J., Xie, L., & Pietrafesa, L. J. (2002). Evidence of the Gulf Stream's influence on tropical cyclone intensity. *Geophysical Research Letters*, *29*(16), 1801. https://doi.org/10.1029/2002GL014920

Brooks, D. A., & Bane, J. M. (1978). Gulf Stream deflection by a bottom feature off Charleston, South Carolina. *Science*, *201*(4362), 1225–1226. https://doi.org/10.1126/science.201.4362.1225

Caesar, L., Rahmstorf, S., Robinson, A., Feulner, G., & Saba, V. (2018). Observed fingerprint of a weakening Atlantic Ocean overturning circulation. *Nature*, *556*, 191–196. https://doi.org/10.1038/s41586-018-0006-5

Cangialosi, J. P., Latto, A. S., & Berg, R. (2018). Hurricane Irma (AL112017) (Tech. rep.). NOAA National Hurricane Center. https://www.nhc.noaa.gov/data/tcr/AL112017_Irma.pdf

Chelton, D. B., & Davis, R. E. (1982). Monthly mean sea-level variability along the West Coast of North America. *Journal of Physical Oceanography*, *12*, 757–784.

Cornillon, P., Stramma, L., & Price, J. F. (1987). Satellite measurements of sea surface cooling during hurricane Gloria. *Nature*, *326*, 373–375. https://doi.org/10.1038/326373a0

Dee, D. P., Uppala, S. M., Simmons, A. J., Berrisford, P., Poli, P., Kobayashi, S., et al. (2011). The ERA-Interim reanalysis: Configuration and performance of the data assimilation system. *Quarterly Journal of the Royal Meteorological Society*, *137*, 553–597. https://doi.org/10.1002/qj.828

Enfield, D. B., & Allen, J. S. (1980). On the structure and dynamics of monthly mean sea level anomalies along the Pacific Coast of North and South America. *Journal of Physical Oceanography*, *10*, 557–578.

Ezer, T., Atkinson, L. P., & Tuleya, R. (2017). Observations and operational model simulations reveal the impact of Hurricane Matthew (2016) on the Gulf Stream and coastal sea level. *Dynamics of Atmospheres and Oceans*, *80*, 124–138. https://doi.org/10.1016/j.dynatmoce.2017.10.006

Galarneau, T. J. Jr., Davis, C. A., & Shapiro, M. A. (2013). Intensification of Hurricane Sandy (2012) through extratropical warm core seclusion. *Monthly Weather Review*, *141*, 4296–4231. https://doi.org/10.1175/MWR-D-13-00181.1

Geisler, J. E. (1970). Linear theory of the response of a two layer ocean to a moving hurricane. *Geophysical & Astrophysical Fluid Dynamics*, *1*(1–2), 249–272. https://doi.org/10.1080/03091927009365774

Gill, A. E. (1982). *Atmosphere-ocean dynamics, international geophysics series* (Vol. 30). San Diego, CA: Academic Press.

Goni, G., Todd, R. E., Jayne, S., Halliwell, G., Glenn, S., Dong, J., et al. (2017). Autonomous and Lagrangian ocean observations for Atlantic tropical cyclone studies and forecasts. *Oceanography*, *30*(2), 92–103. https://doi.org/10.5670/oceanog.2017.227

Gula, J., Molemaker, M. J., & McWilliams, J. C. (2015). Gulf Stream dynamics along the southeastern U.S. seaboard. *Journal of Physical Oceanography*, *45*, 690–715. https://doi.org/10.1175/JPO-D-14-0154.1

Kourafalou, V. H., Androulidakis, Y. S., Halliwell, G. R. Jr., Kang, H., Mehari, M. M., Le Hénaff, M., et al. (2016). North Atlantic Ocean OSSE system development: Nature Run evaluation and application to hurricane interaction with the Gulf Stream. *Progress in Oceanography*, *148*, 1–25. https://doi.org/10.1016/j.pocean.2016.09.001

Large, W. G., & Pond, S. (1980). Open ocean momentum flux measurements in moderate to strong winds. *Journal of Physical Oceanography*, *11*, 324–336.

Lee, T. N., & Williams, E. (1988). Wind-forced transport fluctuations of the Florida Current. *Journal of Physical Oceanography*, *18*, 937–946.

Meinen, C. S., Baringer, M. O., & Garcia, R. F. (2010). Florida Current transport variability: An analysis of annual and longer-period signals. *Deep-Sea Research Part I*, *57*(7), 835–846. https://doi.org/10.1016/j.dsr.2010.04.001

Meinen, C. S., & Luther, D. S. (2016). Structure, transport, and vertical coherence of the Gulf Stream from the Straits of Florida to the Southeast Newfoundland Ridge. *Deep-Sea Research Part I*, *112*, 137–154. https://doi.org/10.1016/j.dsr.2016.03.002

Mooers, C. N. K., Meinen, C. S., Baringer, M. O., Bang, I., Rhodes, R., Barron, C., & Bub, F. (2005). Cross validating ocean prediction and monitoring systems. *Eos Transactions American Geophysical Union*, *86*(29), 269–273. https://doi.org/10.1029/2005EO290002

Nguyen, L. T., & Molinari, J. (2012). Rapid intensification of a sheared, fast-moving hurricane over the Gulf Stream. *Monthly Weather Review*, *140*, 3361–3378. https://doi.org/10.1175/MWR-D-11-00293.1

Oey, L.-Y., Ezer, T., Wang, D.-P., Fan, S.-J., & Yin, X.-Q. (2006). Loop Current warming by Hurricane Wilma. *Geophysical Research Letters*, *33*, L08613. https://doi.org/10.1029/2006GL025873

Ortner, P. B., Lee, T. N., Milne, P. J., Zika, R. G., Clarke, M. E., Podesta, G. P., et al. (1995). Mississippi River flood waters that reached the Gulf Stream. *Journal of Geophysical Research*, *100*(C7), 13,595–13,601. https://doi.org/10.1029/95JC01039

Price, J. F. (1983). Internal wave wake of a moving storm. Part 1: Scales, energy budget and observations. *Journal of Physical Oceanography*, *13*, 949–965.

Rahmstorf, S. (2017). Risign hazard of storm-surge flooding. In *Proceedings of the National Academy of Sciences* (pp. 11,806–11,808). https://doi.org/10.1073/pnas.1715895114

Rudnick, D. L., Davis, R. E., & Sherman, J. T. (2016). Spray underwater glider operations. *Journal of Atmospheric and Oceanic Technology*, *33*(6), 1113–1122. https://doi.org/10.1175/JTECH-D-15-0252.1

Rudnick, D. L., Sherman, J. T., & Wu, A. P. (2018). Depth-average velocity from Spray underwater gliders. *Journal of Atmospheric and Oceanic Technology*, *35*, 1665–1673. https://doi.org/10.1175/JTECH-D-17-0200.1

Sampson, C. R., & Schrader, A. J. (2000). The Automated Tropical Cyclone Forecasting System (Version 3.2). *Bulletin of the American Meteorological Society*, *81*(6), 1231–1240. https://doi.org/10.1175/1520-0477(2000)081<1231:TATCFS>2.3.CO;2

Sherman, J., Davis, R. E., Owens, W. B., & Valdes, J. (2001). The autonomous underwater glider "Spray". *IEEE Journal of Oceanic Engineering*, *26*(4), 437–446. https://doi.org/10.1109/48.972076

Sweet, W. V., Zervas, C., & Gill, S. K. (2009). Elevated east coast sea level anomaly: June–July 2009 (*NOAA Technical Report NOS CO-OPS 051*). Silver Spring, Md: National Oceanic and Atmospheric Association, National Ocean Service, Center for Operational Oceanographic Products and Services.

Theuerkauf, E. J., Rodriguez, A. B., Fegley, S. R., & Luettich, R. A. (2014). Sea level anomalies exacerbate beach erosion. *Geophysical Research Letters*, *41*, 5139–5147. https://doi.org/10.1002/2014/GL060544

Thornalley, D. J. R., Oppo, D. W., Ortega, P., Robson, J. I., Brierley, C. M., Davis, R., et al. (2018). Anomalously weak Labrador Sea convection and Atlantic overturning during the past 150 years. *Nature*, *556*, 227–230. https://doi.org/10.1038/s41586-018-0007-4

Thyng, K. M., Greene, C. A., Hetland, R. D., Zimmerle, H. M., & DiMarco, S. F. (2016). True colors of oceanography: Guidelines for effective and accurate colormap selection. *Oceanography*, *29*(3), 9–13. https://doi.org/10.5670/oceanog.2016.66

Todd, R. E. (2017). High-frequency internal waves and thick bottom mixed layers observed by gliders in the Gulf Stream. *Geophysical Research Letters*, *44*, 6316–6325. https://doi.org/10.1002/2017GL072580

Todd, R. E., & Locke-Wynne, L. (2017). Underwater glider observations and the representation of western boundary currents in numerical models. *Oceanography*, *30*(2), 88–89. https://doi.org/10.5670/oceanog.2017.225

Todd, R. E., & Owens, W. B. (2016). Gliders in the Gulf Stream, publicly available dataset. https://doi.org/10.21238/S8SPRAY2675

Todd, R. E., Owens, W. B., & Rudnick, D. L. (2016). Potential vorticity structure in the North Atlantic western boundary current from underwater glider observations. *Journal of Physical Oceanography*, *46*(1), 327–348. https://doi.org/10.1175/JPO-D-15-0112.1

Todd, R. E., Rudnick, D. L., Sherman, J. T., Owens, W. B., & George, L. (2017). Absolute velocity estimates from autonomous underwater gliders equipped with Doppler current profilers. *Journal of Atmospheric and Oceanic Technology*, *34*(2), 309–333. https://doi.org/10.1175/JTECH-D-16-0156.1

Wright, R. (1969). Temperature structure across the Kuroshio before and after typhoon Shirley. *Tellus*, *21*(3), 409–413. https://doi.org/10.3402/tellusa.v21i3.10096

Wu, C.-R., Chang, Y.-L., Oey, L.-Y., Chang, C.-W. J., & Hsin, Y.-C. (2008). Air-sea interaction between tropical cyclone Nari and Kuroshio. *Geophysical Research Letters*, *35*, L12605. https://doi.org/10.1029/2008GL033942